#141 Dupl

FERMILAB-PUB-73-147-E

#141 Phys. Rev.

Submitted to Physical Review.

ANL/HEP 7354

The Reaction $pp \rightarrow pp\pi^+\pi^-$ at 205 GeV/c*

M. DERRICK, B. MUSGRAVE, P. SCHREINER and H. YUTA
Argonne National Laboratory, Argonne, Illinois 60439

The reaction $pp \rightarrow pp\pi^+\pi^-$ is studied at 205 GeV/c using the 30-inch bubble chamber at the National Accelerator Laboratory. The event selection is discussed in detail and the cross section is measured to be 0.68 ± 0.14 mb. This cross section is higher than one would expect based on a simple power law extrapolation of lower energy data. Peripheral production of a low-mass $p\pi^+\pi^-$ system dominates the reaction. The data are consistent with conservation of t-channel helicity.

*Work supported by the U. S. Atomic Energy Commission.

I. Introduction

The reaction

$$pp \rightarrow pp\pi^+\pi^- \qquad (1)$$

has been extensively studied for momenta from threshold up to 28 GeV/c.[1-4] The data exhibit a pronounced, low-mass enhancement in the $p\pi^+\pi^-$ system with some suggestion of structure corresponding to isospin 1/2 N^* resonance production.[4-5] Although it is generally asserted on the basis of the existence of the low-mass enhancement and its peripheral nature that the reaction exhibits strong diffractive production of the $p\pi\pi$ system, the total cross section for (1) decreases markedly with increasing beam momentum from 10 to 28 GeV/c, whereas diffractive processes should be nearly independent of beam momentum. We present a study of this reaction at 205 GeV/c and find that the cross section decreases more slowly between 28 and 205 GeV/c than is found for incident momenta below 28 GeV/c, which suggests that diffractive processes are becoming dominant in the several hundred GeV energy region.

II. Experimental Details

The data were obtained from a complete analysis of a 50,000 picture exposure of the 30-inch hydrogen bubble chamber exposed to a 205 GeV/c proton beam at the National Accelerator Laboratory (NAL). The results reported here come from measurements of 1191 four-prong events in a fiducial

volume which allows a minimum length of 15 cm for outgoing secondary tracks. About 95% of the four-prong events were successfully reconstructed by TVGP; the other 5% do not represent a significant bias as regards the results presented here. There were 24 events in which no usable curvature information was obtained for two or more secondary tracks. For the remainder, either three- or four-constraint kinematical fits were attempted to hypothesis (1) depending upon whether the event has a fast particle whose curvature was not well determined. In the fit the beam track angles were taken from a set of measured non-interacting beam tracks and the beam momentum was set at the design value of 205 ± 2.0 GeV/c. We found a total of 262 events giving one or more fits to (1), 43 of which were rejected on the basis of ionization density of the slow tracks.

In discussing the purity of the sample, we find that it is frequently important to distinguish between events having three slow and one fast particle in the laboratory (target breakup) and those where this situation is reversed (projectile breakup), since the measurement errors and also the contamination problems are different for the two samples. It is necessary to (a) show that any fits obtained are not biased by incorrect mass assignments; (b) demonstrate that all events which can be expected to satisfy the kinematics of $pp\pi^+\pi^-$ do obtain a fit; (c) confirm that the final fitted sample exhibits the required symmetry of the pp CM system; and (d) to estimate the contamination from events with neutral particles which also give fits to (1).

We first remove an obvious bias occurring for the projectile breakup events arising from incorrect particle assignment. Selecting the fit with the highest chi-square probability in cases of multiple fits, we show in Fig. 1(a) the Feynman x-distribution for the fitted π^+. A pronounced asymmetry between the forward and backward CM hemisphere is obvious with an excess of events having $x \geqslant 0.6$. The Feynman x-distribution for all π^+ in the four-prong events, which are identified by ionization, is shown in Fig. 1(b), where there are clearly very few π^+ with $x < -0.6$. Thus we remove from the sample of kinematical fits events where the x of the fitted π^+ exceeds 0.6, to ensure symmetry in the pp CM system. We completely discard events which only have such a fit and select the fast-forward proton interpretation as opposed to a fast π^+ for events with both types of fits. After this cut, there remains a sample of 191 events.

We next use two missing mass squared distributions obtained from the complete event sample by requiring three particles in the backward and one in the forward CM hemisphere. Ionization is very powerful in identifying most of the target breakup particles which are generally slow in the laboratory. Failing such particle identification, negative tracks are assumed π^- and positive tracks are tried as both π^+ and proton in the case of two unidentified positive curvature tracks. In this latter case, the identification for which the missing mass from the three slowest tracks is nearest to the proton mass is adopted. Fig. 2(a) shows the missing mass from the four charged particles for events where a momentum measurement was possible

for all outgoing tracks. A pronounced, albeit wide, peak is seen close to zero. Fig. 2(b) shows the missing mass from the three "target breakup" tracks. This distribution contains all of the events from Fig. 2(a) as well as the events where the momentum of the fast forward track could not be measured. Again, a pronounced peak appears, this time close to the proton mass squared.

The events in these peaks are candidates for reaction (1). Events giving an acceptable 3C or 4C fit are shown shaded and one sees that no significant loss of fits occurs for this subsample. Fig. 2(c, d) shows the missing mass squared distributions for all events including the projectile breakup sample.[6] The greater background under the peak for the complete sample results from the misassignment of particle mass for some of the events with three fast particles in the laboratory; in particular, the projectile breakup into $n\pi^+\pi^+\pi^-$ when misidentified as $p\pi^+\pi^-$ can give such a spurious peak.

In Fig. 1(c, d, e) we show, for the fitted events, the Feynman x-distributions for the π^+, π^- and p, respectively. There is good overall forward-backward symmetry in each case, and we note that for the complete sample of fitted events, there are 84 events with a 3 to 1 division of particles between the forward and backward hemispheres and 82 events with a 1 to 3 division. The remaining 25 events have a 2 to 2 division. At this stage, we conclude that there is no significant evidence that kinematical fits to (1) are lost, and that the expected symmetry of the pp CM system is adequately satisfied.

A further question is how much contamination is included in the sample from events with neutral particles. We have studied this in several ways. First, we have considered the stability of the fits to the presence of a pion by deleting the negatively charged particle and attempting the fit $pp \rightarrow pp\pi^+$. In 12 of the 82 events fitting (1), with three particles in the backward and one in the forward CM hemisphere, this attempt was successful indicating the fits are quite sensitive to a π^o at the target vertex.

However, the case in which a π^o is associated with the fast leading particle is clearly more difficult to kinematically discriminate against in view of the width of the missing mass peak in Fig. 2(b). From consideration of the symmetric events in which there is a $n\pi^+$ or $p\pi^o$ system in the backward hemisphere and three-charged particles in the forward hemisphere, we find that such "double diffraction" events are rare. By reflecting the momentum vectors of the slow π^+ or proton, as the case may be, to the opposite CM hemisphere, we can compare the longitudinal laboratory rapidity distribution of these events with the same distribution for the events fitting hypothesis (1). We thereby estimate a background of 20 ± 5 events from the "double-diffraction" type events.[7]

We have also studied the contamination in the projectile fragmentation sample by measuring those six-prong events which have a slow proton identified by ionization and a system of missing-mass squared ≤ 20 GeV^2 recoiling from it. We deleted two prongs at a time in each of these events and tried to fit the remaining tracks to hypothesis (1). Assuming that these events are

kinematically similar to actual four-prong events with one or more missing π^o's, we find that the contamination from this source in our four-prong $pp\pi^+\pi^-$ fits to be 23 ± 7 events.

Finally, we note that of the events giving a kinematical fit to (1), there are two events known to have an associated K_s^o and one event with a possible associated γ conversion, although this could not be checked by measurement because of its very low energy. Observation of these K_s^o events implies the presence of ~ 6 other events with a K^o in the sample. Since the average γ conversion probability is only 0.018, observation of at most one photon conversion associated with the events kinematically fitting (1), while encouraging, by no means guarantees lack of background from events with one or more π^o.

III. Results

Combining the contamination studies, we measure the total cross section for reaction (1) to be 0.68 ± 0.14 mb, where the error assignment includes our estimate of the possible multi-neutral contamination. The fraction of this cross section which corresponds to target fragmentation (three particles in the backward hemisphere) is 0.29 ± 0.06 mb. In Fig. 3 we show the variation of the production cross section for (1) with laboratory momentum;[1-4] the dashed curve in the figure is an extrapolation of the fit of p_{lab}^{-n} to the 10-28 GeV/c data. We note that our cross section is significantly higher than this extrapolation would indicate. This suggests the presence of a dominant Pomeron exchange contribution to the reaction. Of course, since

our 205 GeV/c result is ~ 0.4 mb less than the 28 GeV/c result, a less steep momentum dependence of the cross section at higher momenta is also an acceptable explanation. To decide between these two possibilities requires data at other high momenta.

A dominant feature of the data is the production of a low $p\pi^+\pi^-$ effective mass enhancement. Fig. 4 shows a scatter plot of the two $p\pi^+\pi^-$ effective mass combinations for each event. There are very few mass combinations not associated with either the forward or backward produced enhancement. There is clearly no evidence for the production of any high mass N^* resonances. In fact, the shape of the $p\pi^+\pi^-$ mass distribution, selecting the smallest value for each event (Fig. 5(a)), is quite similar to that seen at lower energies. The mass resolution is good for the target breakup events (~ 10 MeV), but the small number of events precludes a search for fine structure in the low-mass enhancement. Although the constraint of small $p\pi\pi$ mass also requires small $p\pi^+$ and $p\pi^-$ effective masses, it is clear from Fig. 5(b, c) that the $\Delta^{++}(1236)$ is a much more prominent intermediate state than is $\Delta^{o}(1236)$.

The four-momentum transfer squared (t) distribution between the target (projectile) and the $p\pi^+\pi^-$ system is very peripheral. Fig. 6 shows the combined forward and backward CM data for $p\pi^+\pi^-$ effective mass less than 3 GeV. We have fit the data to the form Ae^{Bt} and find that the slope of the distribution is $9.2 \pm 1.1\ (\mathrm{GeV/c})^{-2}$ for $0.0 \leq |t| \leq 0.30\ (\mathrm{GeV/c})^2$. This is only slightly smaller than that measured for pp elastic scattering in this

experiment,[8] and is further evidence that reaction (1) is dominated by Pomeron exchange.

If the production of the low-mass $p\pi^+\pi^-$ system is indeed a diffractive process, it is of interest to test for the presence of s-channel or t-channel helicity conservation.[9] Low energy data[4] on reaction (1) have suggested that it is t-channel helicity which is conserved. We have studied the azimuthal angular distributions in the $p\pi^+\pi^-$ rest frame of the normal to the $p\pi^+\pi^-$ production plane (ϕ_N), the decay proton direction (ϕ_P), and the decay Δ^{++} direction (ϕ_Δ). A necessary condition for helicity conservation is isotropy of the three distributions in the appropriate coordinate system. Fig. 7 shows the azimuthal distribution in the s- and t-channel systems. Two of the s-channel distributions, for the proton and Δ^{++} (Fig. 7(b, c)), show anisotropy (χ^2/DF = 3.21 and 2.99 respectively). However, all three t-channel distributions (Fig. 7(d-f)) are reasonably isotropic (χ^2/DF = 1.79, 1.30 and 0.91, respectively). We conclude that our 205 GeV/c data are consistent with the observation at lower momentum that t-channel helicity is being conserved in the diffractive production of the $p\pi^+\pi^-$ system.

The cooperation of the NAL staff in obtaining this exposure is gratefully acknowledged, as is also the work of the Argonne scanning group.

References

1. "Compilation of Cross Sections I; Proton-Induced Reactions," CERN/HERA 70-2 (1970).

2. "NN and ND Interactions (Above 0.5 GeV/c) - A Compilation," UCRL-20000 NN (1970).

3. U. Idschok et al., Nucl. Phys. B53, 282 (1973).

4. J. G. Rushbrooke et al., Phys. Rev. D4, 3273 (1971).

5. J. G. Rushbrooke in Proceedings of the 14th International Conference on High Energy Physics, edited by J. Prentki and J. Steinberger (European Organization for Nuclear Research, Geneva, 1968) p. 158.

6. We note that for 14 of the 191 fitted events, the positively charged particles' mass assignments used in the missing mass calculations differ from the "correct" assignments obtained in the fits. However, this does not change any of our conclusions.

7. Further discussion of these background events is given in "Diffraction Dissociation in pp Interactions at 205 GeV/c," M. Derrick et al., ANL/HEP 7332, submitted to the American Physical Society Meeting at Berkeley, California (1973).

8. S. Barish et al., ANL/HEP 7337, submitted to Phys. Rev. D.

9. In the s-channel, the z-axis is along the $p\pi^+\pi^-$ direction in the overall CM system; in the t-channel, the z-axis is along the incident proton

direction in the $p\pi^+\pi^-$ rest system. Both coordinate systems are right-handed with the y-axis along the normal to the production plane.

Figure Captions

Fig. 1 The distribution of the Feynman x variable, $x = 2p^*_{\parallel}/\sqrt{s}$ where $p^*_{\parallel}$ and $\sqrt{s}$ are the particles' longitudinal CM momentum and the total energy in the CM system, respectively, for: (a) the fitted π^+ in $pp \rightarrow pp\pi^+\pi^-$, (b) the measured π^+ from all four-prong events where the π^+ is identified by ionization - the histogram to the right of the dotted line corresponds to the right-hand ordinate scale, (c, d, e) the π^+, π^- and p from $pp\pi^+\pi^-$ fits after removing those with $x_{\pi^+} \geqslant 0.6$.

Fig. 2 (a) The distribution in missing mass squared (MM^2) from the $pp\pi^+\pi^-$, for events with $p\pi^+\pi^-$ in the backward CM hemisphere. Events giving a 4C fit to this final state are shown shaded, (b) the distribution in MM^2 from $p\pi^+\pi^-$ where these are the three lowest momentum tracks in the event and are in the backward CM hemisphere. The events giving either 3C or 4C fit are shown shaded; (c) as in (a) but for all four-prong events; (d) as in (b) but for all four-prong events.

Fig. 3 The production cross section for the reaction $pp \rightarrow pp\pi^+\pi^-$ as a function of laboratory momentum.

Fig. 4 Scatter plot of the two $p\pi^+\pi^-$ effective mass combinations per event; p_F and p_S identify the fast and slow protons of each event.

Fig. 5 The effective mass distribution of (a) the $p\pi^+\pi^-$ system, selecting the smallest for each event, (b) the $p\pi^+$ system, and (c) the $p\pi^-$ system.

Fig. 6 The four-momentum transfer squared distribution between the target (projectile) and the $p\pi^+\pi^-$ system for $p\pi^+\pi^-$ mass less than 3 GeV.

Fig. 7 Azimuthal decay angular distribution in the s-channel coordinate system of (a) the normal to the $p\pi\pi$ system, (b) the proton, and (c) the Δ^{++}; azimuthal decay angular distribution in the t-channel coordinate system of (d) the normal to the $p\pi\pi$ system, (e) the proton, and (f) the Δ^{++}.

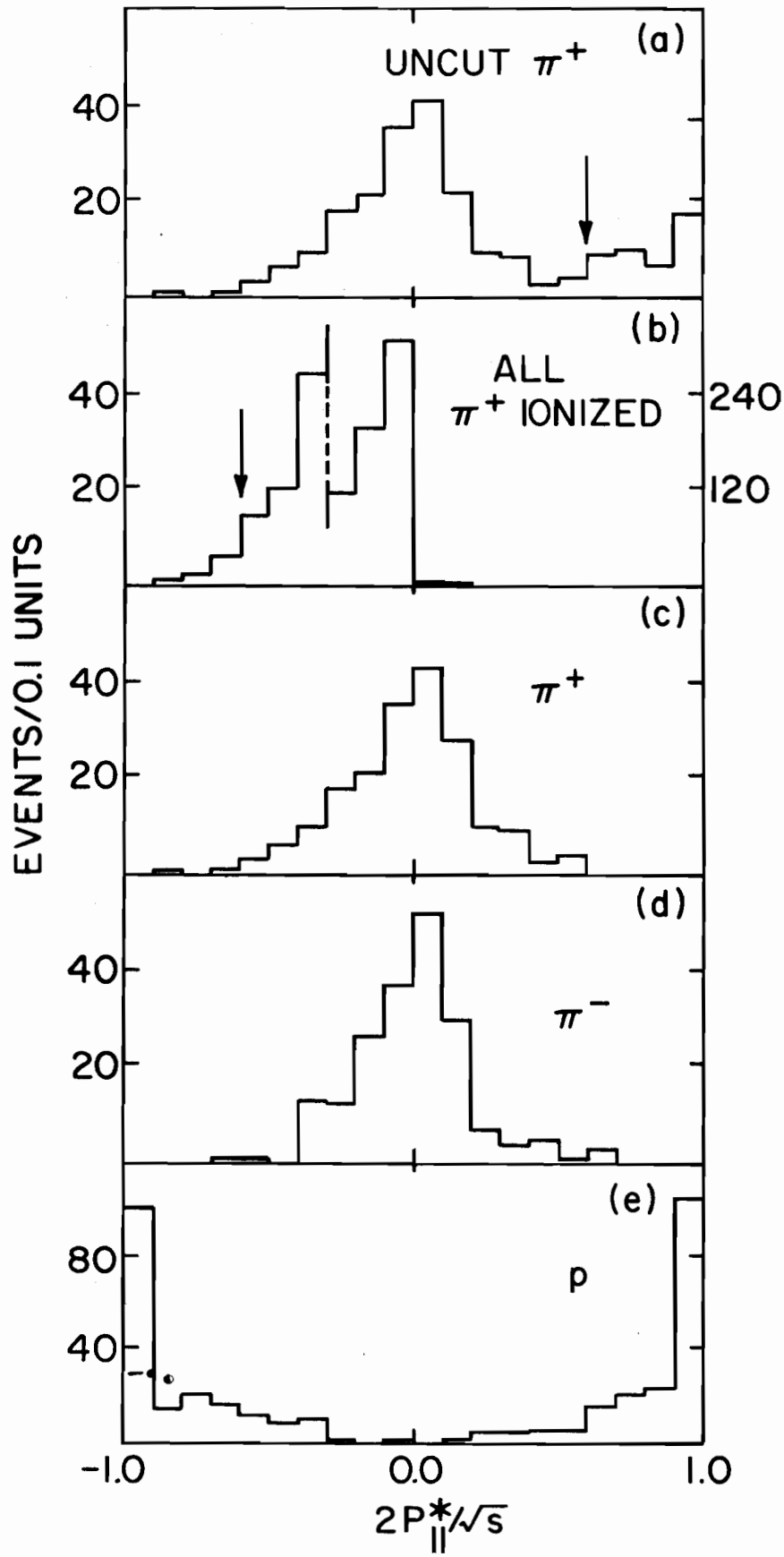
(a)
UNCUT π^+
40
20
(b)
ALL
π^+ IONIZED
240
120
40
20
(c)
π^+
40
20
(d)
π^-
40
20
(e)
p
80
40
EVENTS/0.1 UNITS
-1.0
0.0
1.0
$2P^*_{\parallel}/\sqrt{s}$

Fig. 1

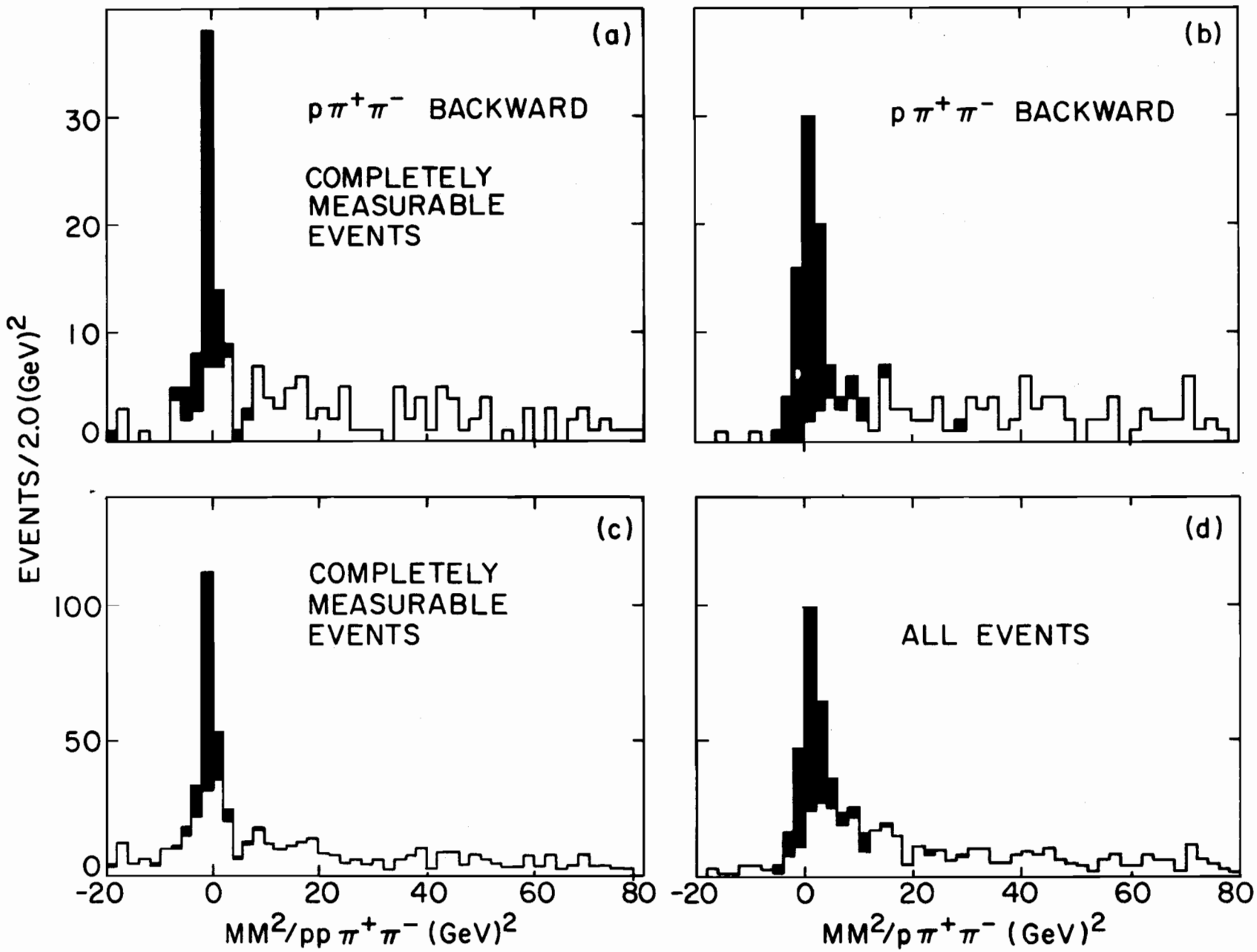
(a)
$p\pi^+\pi^-$ BACKWARD
COMPLETELY MEASURABLE EVENTS
(b)
$p\pi^+\pi^-$ BACKWARD
(c)
COMPLETELY MEASURABLE EVENTS
(d)
ALL EVENTS
EVENTS/2.0(GeV)^2
0
10
20
30
50
100
-20
0
20
40
60
80
$MM^2/pp\pi^+\pi^-$ (GeV)^2
$MM^2/p\pi^+\pi^-$ (GeV)^2

Fig. 2

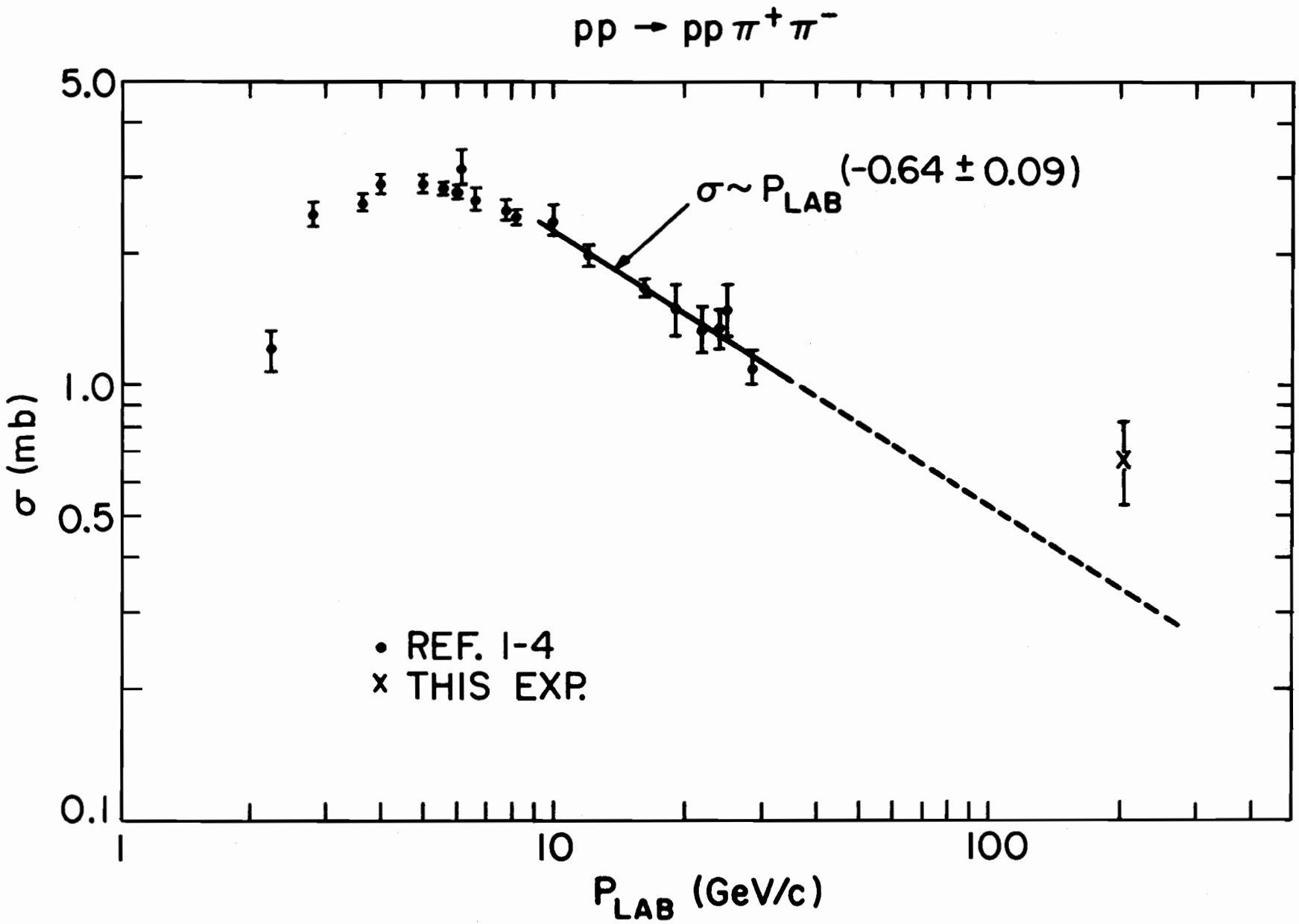
pp → pp π⁺π⁻
5.0
1.0
0.5
0.1
σ (mb)
σ ~ P_LAB (-0.64 ± 0.09)
• REF. 1-4
× THIS EXP.
1
10
100
P_LAB (GeV/c)

Fig. 3

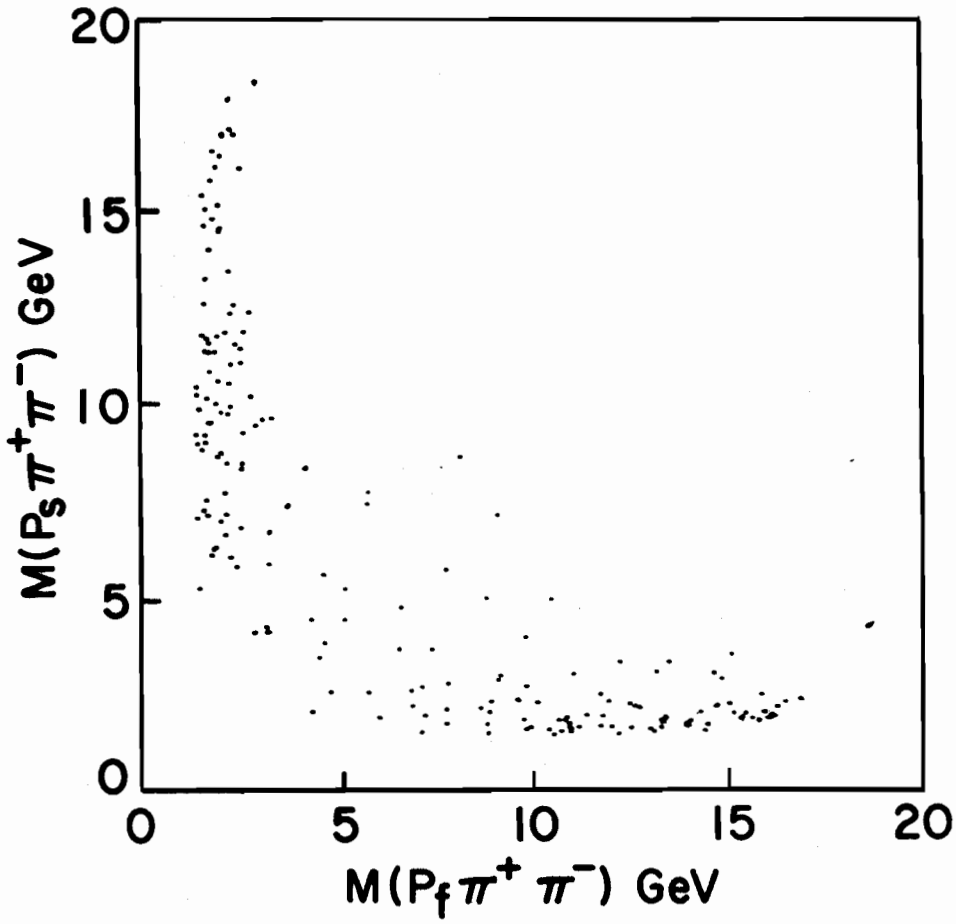

Fig. 4

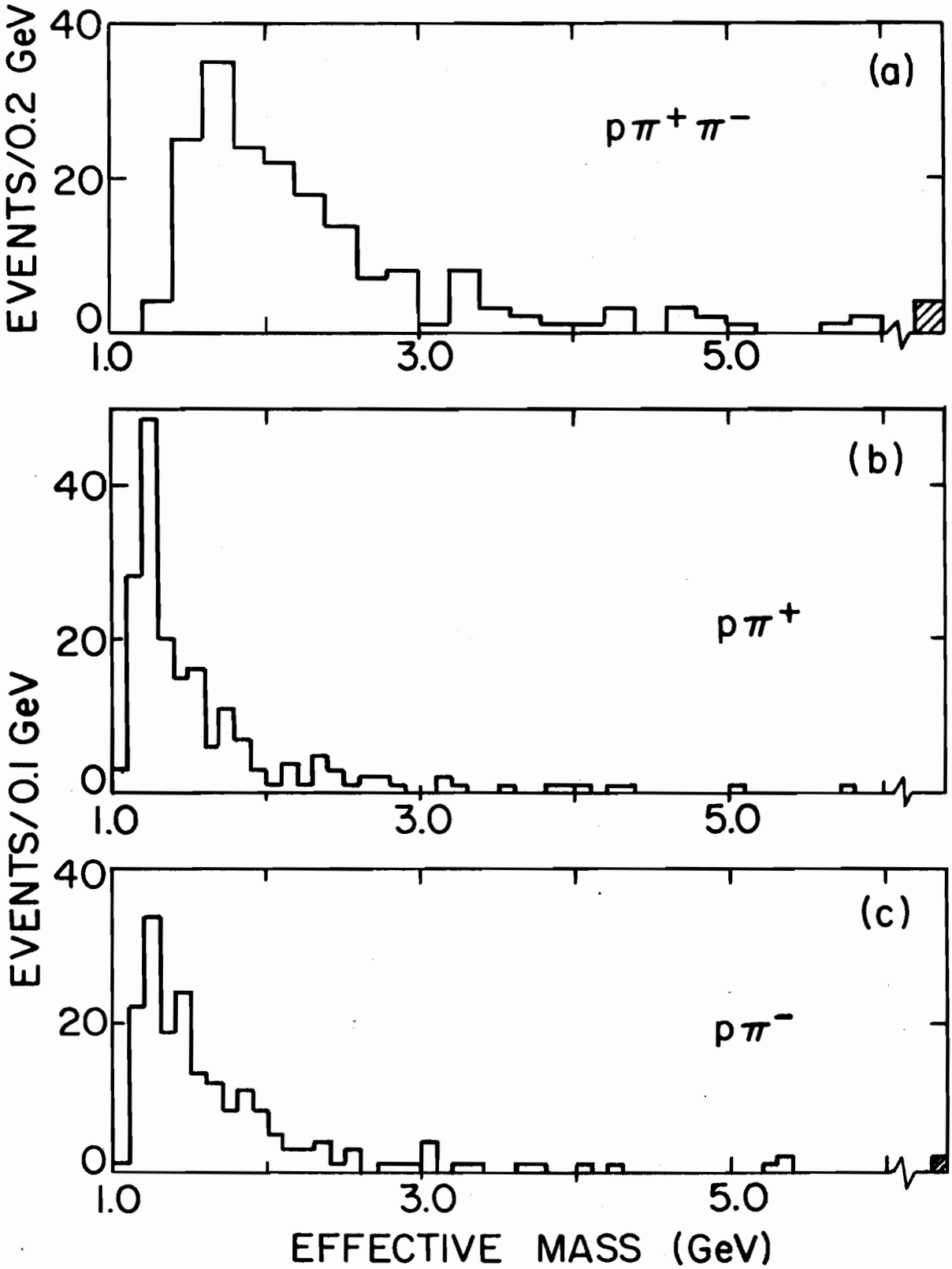
EVENTS/0.2 GeV
40
20
0
1.0
3.0
5.0
(a)
$p\pi^+\pi^-$
EVENTS/0.1 GeV
40
20
0
1.0
3.0
5.0
(b)
$p\pi^+$
40
20
0
1.0
3.0
5.0
(c)
$p\pi^-$
EFFECTIVE MASS (GeV)

Fig. 5

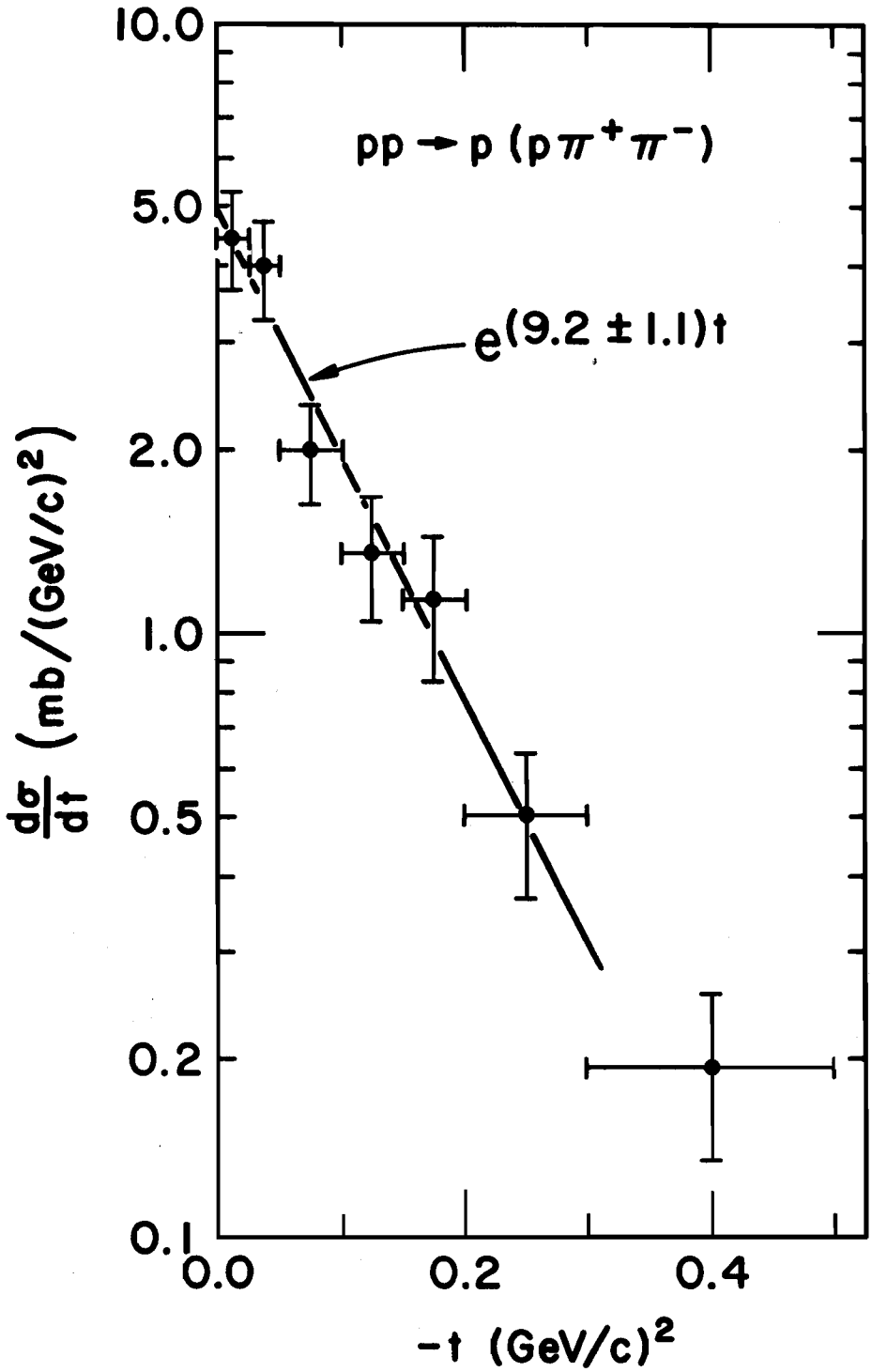
10.0
5.0
2.0
1.0
0.5
0.2
0.1
0.0
0.2
0.4
pp → p (pπ⁺π⁻)
e(9.2 ± 1.1)t
dσ/dt (mb/(GeV/c)²)
-t (GeV/c)²

Fig. 6

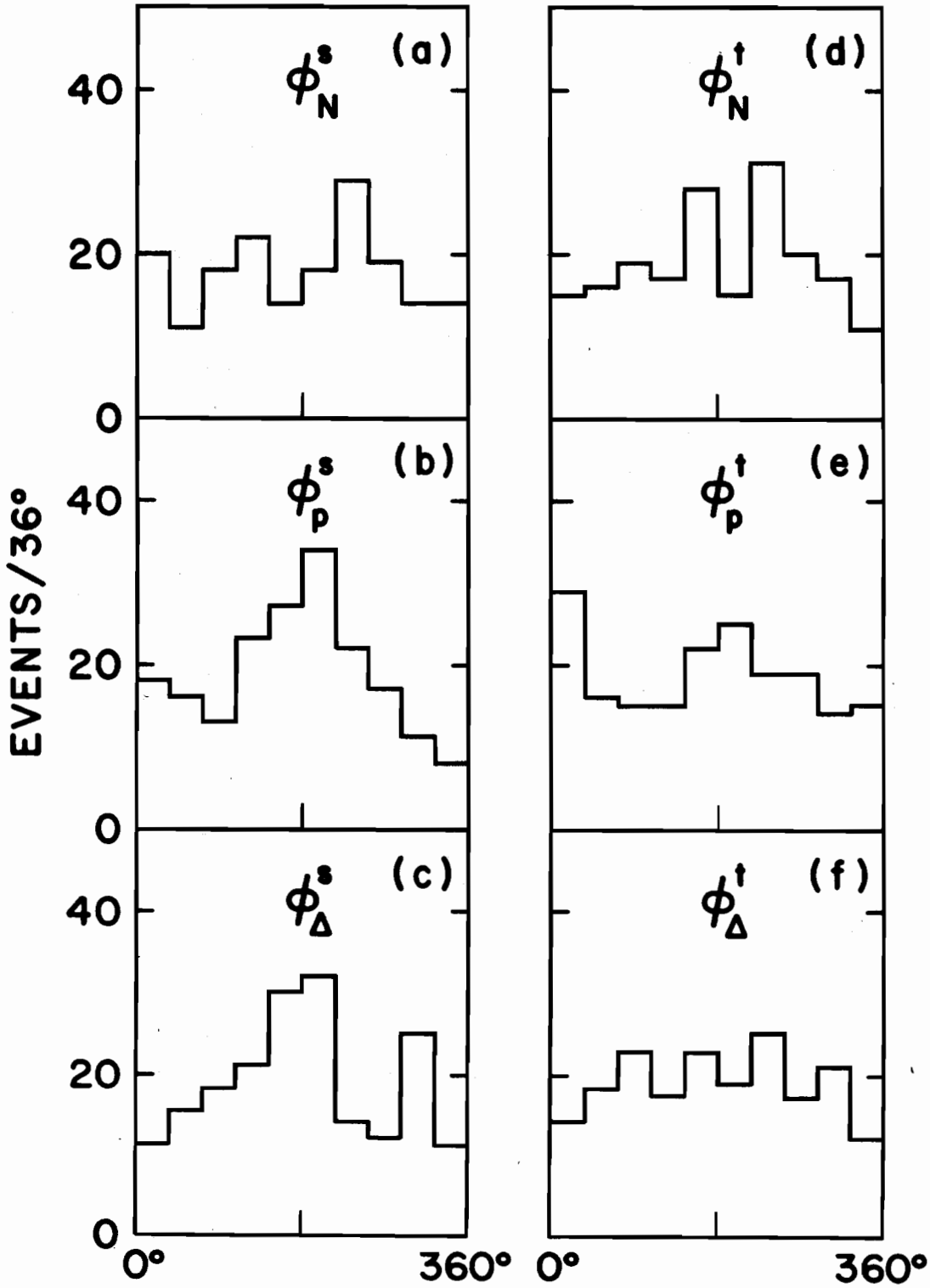
EVENTS/36°
40
20
0
(a)
ϕ_N^s
(b)
ϕ_p^s
(c)
ϕ_Δ^s
(d)
ϕ_N^t
(e)
ϕ_p^t
(f)
ϕ_Δ^t
0°
360°
0°
360°

Fig. 7